Solar Energy 164 (2018) 77–88

Contents lists available at ScienceDirect

Solar Energy

journal homepage: www.elsevier.com/locate/solener

Ocular risks assessment in a central receiver solar power facility based on measured data of direct solar radiation

Danyela Samaniego Rascón[a,*], Almerindo D. Ferreira[a], Manuel C. Gameiro da Silva[a], Cuitlahuac Iriarte[b]

[a] ADAI, LAETA, Department of Mechanical Engineering, University of Coimbra, Rua Luis Reis Santos, 3030-788 Coimbra, Portugal
[b] PSH, Department of Industrial Engineering, Universidad de Sonora, Blvd. Luis Encinas y Rosales S/N, Col. Centro, Hermosillo, Sonora, Mexico

ARTICLE INFO

Keywords:
Solar energy
Central receiver systems
Risk assessment
Ocular exposures

ABSTRACT

Among the Concentrated Solar Power technologies, central receiver systems (CRS) is the technology moving to the forefront in market penetration. CRS requires the use of heliostats oriented toward the central receiver in order to concentrate solar radiation. The excess of light due to the reflection of the sunlight on the heliostats' surface and the brightness of the receiver are considered as possible situations of risk for the eye. The paper briefly outlines the physiological response to solar radiation subjected to momentary ocular exposures. This will be followed by the description of health impairments and the presentation of the methodology and safety doses. A case of study based on direct solar radiation measurements, is foreseen. Two scenarios were evaluated, the action of seeing directly to a heliostats' surface and the action of seeing the reflected radiation from the receiver. In the case of seeing the brightness from receiver, there exist a low potential to cause a temporary effect on the eye. Besides, a person that is looking at heliostat surface has a huge potential to present a temporary effect (after-image). The final section of the study will present and discussed the results obtained from the analysis of the case of study and provide some recommendations. The investigation aims to contribute with information directed to environmental scientists, standard developers and the solar industry that could improve/develop safety procedures directed toward the occupational health and safety within solar energy applications.

1. Introduction

Due the environmental problems due to pollutants that are released into the atmosphere and the scarcity of fossil fuels, renewable sources of energy seems to be an attractive solution for power supply (Burlafinger et al., 2015; Jamel et al., 2016; Reyes et al., 2016). Governments around the world are working in the implementation of policies that aim to promote the usage of renewable resources for energy production (Corona et al., 2016).

Among the renewable energy systems, Solar energy is considered as a promising option for energy production due to its abundance, zero pollution and economical energy source costs (Ashouri et al., 2015; Astolfi et al., 2017; Mekhilef et al., 2011; Sindhu et al., 2016). The industrial applications of solar energy are distributed into two main categories: the photovoltaic (PV) and the concentrated solar power (CSP) (Mekhilef et al., 2011; Zhao et al., 2017). According to the International Renewable Energy Agency the CSP technologies are increasing in scientific and commercial attention (Corona et al., 2016).

The CSP power plants (also named concentrating solar power or concentrated solar thermal) are based on the concept of solar radiation concentration converted to high temperature thermal energy through direct or indirect operation of a turbine and electricity generator (Gauché et al., 2017; Hamilton, 2011; IEA, 2014; Zhao et al., 2017).

Among the CSP technologies that are dominating the market, are the parabolic through and the central receiver systems (CRS) (Behar et al., 2013; Gauché et al., 2017). Even though at the end of 2016 about 600 MWe (~13%) of nearly 5 GWe of operational CSP capacity worldwide was from CRS, researchers and developers are up to find the path in achieving higher efficiency and lower costs. As a result CRS technologies are more often being developed (Ho, 2017).

Basically CRS uses multiple sun tracking mirrors called heliostats concentrate the sunrays by reflected them on one point, called receiver. The generated heat is used to produce steam from heating fluids. The steam drives a turbine connected to an electrical generator that produces electricity (Kalogirou, 2009; IEA, 2014).

Franck et al. (2009) classified the solar light reflections from the

* Corresponding author.
E-mail addresses: danyela.samaniego@efs.uc.pt (D. Samaniego Rascón), almerindo.ferreira@dem.uc.pt (A.D. Ferreira), manuel.gameiro@dem.uc.pt (M.C.G. da Silva), ciriartec@gmail.com (C. Iriarte).

https://doi.org/10.1016/j.solener.2018.02.034
Received 18 September 2017; Received in revised form 12 December 2017; Accepted 12 February 2018

Nomenclature

f	focal length of the eye (m)
ρ	reflection coefficient
β	total beam divergence angle (mrad)
τ	transmittance coefficient
ω	subtended angle from the source (mrad)
ω_{spot}	subtended angle of the reflected image on a mirror as observed from a given distance (mrad)
A_{spot}	area of the reflected image on a surface viewed by the observer (m^2)
A_p	area of the pupil (m^2)
A_{equiv}	equivalent area of the $\boldsymbol{n}$ heliostats (m^2)
A_{obs}	area seen by the observer (m^2)
A'	area of the reflecting surface (m^2)
b	focal length (m)
C	concentration ratio
D_h	effective diameter of the mirror (m)
d_{spot}	reflecting area of the mirror (m)
d_s	source size (m)
d_p	daylight adjusted pupil diameter (m)
d_r	diameter of the image projected onto the retina (m)
E_{beam}	beam irradiance (W/cm^2)
E_c	irradiance in outside the cornea (W/cm^2)
E_{DNI}	direct normal irradiance at the earth's surface (1000 W/m^2)
E_{equiv}	equivalent Irradiance of the $\boldsymbol{n}$ heliostats (W/cm^2)
E_r	retinal irradiance (W/cm^2)
E_{ref}	reflected irradiance (W/cm^2)
$E_{r,\,burn}$	retinal burn threshold (W/cm^2)
$E_{r,\,flash}$	potential after-image threshold (W/cm^2)
E'	irradiance of the reflecting surface (W/cm^2)
r	distance between the eye and the source (m)
r_{obs}	location of the observer (m)
x	distance (m)

receiver and the heliostats within CRS installations in some different human-interacting scenarios: the reflection directly to the sky (potential risk for airplane pilots), non-concentrated reflection from one single heliostat (potential risk for a person standing in front of the mirror), concentrated solar radiation from the heliostats field (potential risk for workers located in the solar tower) and the reflected solar radiation from the receiver (potential risks for people outside the heliostats field although in the nearby, i.e. car drivers passing in nearby roads, neighbors or pedestrians). Other scenarios were added by Ho et al. (2011), such as the diffuse radiation from the receiver, or the reflection from the mirrors when they are moving from the standby mode or when they are not orientated toward the receiver.

Also, a CRS facility, in order to take the highest advantage of solar energy, has to be submitted to regular cleaning and maintenance of heliostats surfaces, as those activities will allow the maximum reflectivity to achieve the highest productivity level. The cleaning activities can be rather accomplished by a cleaning system based on wet brushing (robot) or/ and by manual activities when it may be required (ECLIMP Termosolar, 2016; Kattke and Vant-Hull, 2012; SENER, 2011).

The CSP facilities are, as expected, commonly located in sunny environments characterized by a high solar ultraviolet index (Franck et al., 2009). Solar radiation, composed by three types of Non-ionizing radiation (UV, VL and IR) according to its wavelength, could interact with the biological system. The biological effect is produced by a change that can be measured after the introduction of some stimuli. Even though it does not necessarily suggest the presence of health hazards, those changes in the biological system could end in detectable impairments. Those changes could influence at physiological, biochemical or behavioral level in individuals. Prolonged human exposure to solar UV radiation may result in acute and chronic health effects on the skin, eye and immune system (Kwan-Hoong, 2003). Carrasco (2003) described at least five types of damages to the eye and skin due to exposure to natural visible light.

The approach needs to be centered in the proper usage of solar energy as developed alternative for power generation, so the outcome could be the expected one (Oncel, 2017). Therefore, analyzing the environmental conditions and addressing the safety at work of such a growing industry is a responsibility of the scientific energy community.

This paper aims to contribute to contribute with crucial information about ocular exposures to solar radiation. It includes a brief outline of solar effects on eyes subjected to momentary exposures followed by the presentation of safety doses and the methodology about the evaluation of specular reflections from the surface of the heliostats and diffuse reflections from the receiver. Following by the assessment of eye hazards in a CRS, which is based on solar radiation measurements and is represented as a case of study. At the end of the last section, the results obtained from the analysis of the case of study are presented and discussed.

The main objective is to contribute with information directed to environmental scientists, standard developers and the solar industry that could provide to improve/develop procedures manual directed toward the occupational health and safety.

1.1. Physiological response to solar radiation: Occupational health effects on eyes

The human eye has the natural aversion response against bright light sources. This response protects it from getting injured by viewing bright sources like the sun. Since this aversion limits, the duration of exposure lasts a fraction of a second (around 0.25 s) (Sliney, 1994). It means that the eye will naturally avoid the bright source by blinking or/and the person will instinctively shift his view from the bright source in order to minimize incident visible light (Franck et al., 2009). In solar radiation exposures, the variation in eyelids opening plays a major role in terms of impact. The eyelids control the amount of light that enters into the eye. For example, the lids are more open during cloudy days as the irradiance is reduced due to the cloud cover. Ocular exposure is affected by the geometry of exposure, which means that sun irradiance reaching the eye is near limited to the indirect radiation that has been diffusely scattered by the atmosphere and reflected from all the surfaces (Vecchia et al., 2007).

Besides, the unforeseen incidence of flash light on a visual scene naturally attracts the attention which could distract someone from his/her ongoing task and/or produce a shock and panic reaction (Toet et al., 2013).

Even though the avoidance instinct of the eye, the intensity of the bright light source, time of exposure, incidence of the exposure and flickering pattern of light might cause temporary and permanent effects (Ho, 2011; Toet et al., 2013). The visual disturbances could appear as a result of the neural processing in the retina after light has been absorbed by the photoreceptors (Toet et al., 2013).

There are several effects (physiological and psychological) that could represent a temporary impact or a permanent damage according to the type of wavelengths that define light intensity absorbed by the retina of the eye.

1.1.1. Temporary effects

Glare is the temporary incapability to see details in the area around a bright light (visual field). Sometimes is called dazzle, being known as the first eye reaction to bright light (Franck et al., 2009). It is not

classified as biological damage because it lasts only as long as the bright light exists within the individual's visual field (Toet et al., 2013). Glare, relative to the ambient lighting, is defined as a result of the exposure to source of continues excessive brightness while glint is attributed to a momentary flash of light (Ho et al., 2011).

1.1.1.1. Disability glare. The moment that glare impact vision is called disability glare, which is caused by the diffractions and scattering of light inside the eye. It is also called physiological glare and it reduces the visual performance (Osterhaus, 2005). The light that is scattered overlays the retinal image and, consequently, reduces the visual contrast. The result of the overlaying scattered light distribution is usually called veiling luminance.

Veiling luminance is the decrement of contrast in the scene in the human eye (Toet et al., 2013). Workers under the presence of disability glare immediately notice the reduction in their ability to see and/or to perform a visual task (Osterhaus, 2005).

1.1.1.2. Discomfort glare. Discomfort glare, also called psychological glare, does not necessarily affect the visual performance but it produces discomfort. An individual under discomfort glare might not notice any negative impact in his work performance but can experience side effects after a period of time, such as headache (Osterhaus, 2005).

1.1.1.3. Flash blindness. The retina adapts physiologically to light and when the light is more intense than that amount at which the retina is adapted at that moment, a temporary and immediate loss of vision is produced. Flash blindness is produced by the bleaching of the retinal visual (light-sensitive) pigments caused by bright light exposures (Franck et al., 2009; Ho et al., 2009; Toet et al., 2013). Most of the people have experienced flash blindness after viewing a flash light from a camera (Ho et al., 2009). Dazzle and the "after-image" effects are the physiological responses to flash blindness (Franck et al., 2009)

1.1.1.4. After-image. The after-image is a temporary scotoma (blind spot), or a lasting image, after looking directly at a bright source as the sun. It is caused by the visual impression which lasts after the image has disappeared. The after-image effect persists from several seconds to several minutes in the visual field in which target spots are partly and/or completely buried. These blind spots are stuck and move with the eye sight. The time to blind spots fade depends on the level of brightness and duration of the light insult, among other factors, such as target contrast, color, size, observer age, and the total adaptation state of the visual system (Franck et al., 2009; Toet et al., 2013).

Effects such as after-image, flash blindness and veiling can be product of experiencing disability glare caused by solar glare. Meanwhile, retinal burn can occur with exposure to concentrated sunlight and solar retinitis with associated scotoma results from staring at the sun (Sliney, 1994).

The prolonged exposures to some of these effects, such as discomfort glare and disability glare, can lead to side effects like headaches and/or other physiological impacts, and reduction of the visual performance (Ho et al., 2014). Glare and flash blindness might be followed by irreversible impairments such as thermal lesions (Toet et al., 2013).

The recovery time, strongly dependent on the brightness of the projected image, ranges from 0.8 to 2.7 s, for approximately 1–3 W/m^2 of solar irradiance at the eye (Franck et al., 2009; Saur and Dobrash, 1969).

For the evaluation of the repercussion effects on a viewer located in the installations of a solar power facility, it is necessary to take into consideration that the effects are directly related to the ambient and background light conditions. In day light conditions flash blindness is not considered to be a problem since the locations usually have bright surroundings and high global and diffuse radiation (Franck et al., 2009).

1.1.2. Reversible and permanent damages

Exposures to solar radiation, mostly UV radiation, are associated with a variety of impairments on cornea, lens and retina. The health disorder depends on the amount and wavelength of radiation that reaches the internal structure of the eye (Diffey, 1991; ICNIRP, 2010; Vecchia et al., 2007). For example, viewing intense VL radiation can be potentially risky for the retina and intense UV can be hazardous for the cornea and lens (Sliney, 2001).

The principal hazard resulting from looking directly at the sun is photoretinitis (solar retinitis with scotoma) which is a retinal damage. Intense exposure to short-wavelength of light can cause thermal lesions, which are burns of the retinal tissue that result in permanent scotomas (Sliney, 1994, 2001; Toet et al., 2013).

Even though the retina is normally enough protected by the cornea and crystalline lens against health effects (less than 1% of UV-A is available to reach the retina), solar retinitis is the consequence of a photochemical injury mechanism subsequent to the exposure of the retina to shorter wavelengths in the visible spectrum (ICNIRP, 2004; Sliney, 1994, 2001). Photoretinitis may result from viewing an extreme bright light for a short period of time or it could be the result of looking at lesser bright light source for longer periods of exposure.

Studying the physiology of the retina, light damage and the renewal process of the retina had been the concern between the adverse impacts to UV-A, and blue light upon the retina (Sliney, 2001).

On the other hand, the cornea does not pass through an adaptation process (increment in the capacity of protection) due to repeated exposures; therefore it is equally vulnerable day after day to the same amount of radiation (ICNIRP, 2010; Knave et al., 2001; Vecchia et al., 2007).

Acute effects such as photokeratitis and photokeratoconjunctivitis are produced by an inflammatory reaction in the cornea and the conjunctiva, respectively, and both can be very painful but don't result in a permanent damage. They appear a few hours after the exposure and last one or two days (Knave et al., 2001). Other effect upon unprotected eyes exposures to sun is fibrous ingrowth of the cornea's tissue (pterygium). Other effects could be attributed to a nonmalignant tumor in the conjunctiva (pingueculum) and cataracts (opacity of the lens). Usually cataracts that eventually lead to blind eye appearance in individuals depend on the age and sun exposure (mostly UV-B exposures) (Diffey, 1991; Vecchia et al., 2007; WHO, 2002).

Risks from glint and glare from bright sources within concentrating solar power plants include the potential of permanent damage in the eye and also temporary effects. Those effects could impact in people within the facility and also in the surroundings (working nearby, pilots flying overhead or motorist driving alongside the site). Assess the potential hazards coming from the glint and glare in concentrating solar power plants is an important requirement to ensure public safety (Ho et al., 2011).

1.2. Previous studies

Several studies investigated the impact of solar radiation reflections of visual sources at solar thermal power plants.

Saur and Dobrash in 1969 published the study about visual inspection of sun reflections from metal surfaces in order to calculate the duration of afterimage disability in automobile drivers. The results showed the need of curvature in mirrors surfaces and matte surfaces in the receiver for the reduction of the glint and glare.

Years later in 1977, Young, developed a research emphasizing on hazards associated with reflecting concentrated solar energy from the receiver in the experimental installations of Sandia National laboratories in Albuquerque, New Mexico. In the same year and same installations, Brumleve (1977) carried on an investigation about eye hazards associated with concentrated reflected light of single and multiple coincident heliostat beams. The results showed that the irradiance of a single heliostat exceeds the safety limits within a short focal distance

(up to 40 m), even though, the safe limits for retina damage were never exceeded in heliostats with focal lengths of more than 270 m.

Almost four decades later Ho et al. (2009) presented a compilation of previous assessments about glint and glare effects, and optical risks in the different CSP technologies. The study resumes the metrics used to determine safe retinal irradiance exposures in order to avoid the permanent eye damage. In addition the authors suggested additional quantitative metrics that could be used for glint and glare analysis in concentrating solar thermal power plants with eye hazards prevention purposes.

One year later, Franck et al. (2009) analyzed potential risks for skin and eyes due to exposure to brightness of the reflected sunlight from the heliostats and the receiver. The authors explored the operation and design features of a central tower installation (facility with 1600 heliostats approximately) in Israel. Through analyzing the potential effects in human health and the safety metrics for the evaluation, the authors conclude with some recommendation for eyes and skin.

In 2011, Ho, evaluated potential glint and glare hazards during short-term exposures from the concentrating solar collector's field at the National Solar Thermal Test Facility (NSTTF). The study basically evaluated the potential for permanent eye injury (retinal burn) and temporary visual impairment (after-image) using Digital photographs of the glare to quantify the irradiance flux in each pixel. The results revealed a strong glare could be observed from the surface of the heliostat over 1700 m (> 1 mile) away when the heliostats were placed in a standby mode; with an aim point ~30 m to the east of the top of the tower. After viewing the glare source directly, a temporary after-image effect was experienced.

In the same year, Ho, in collaboration with Ghanbari and Diver (2011) proposed an analytical model for the evaluation of the specular reflections in point- focus collectors and line-focus collectors, and diffuse reflections (receiver surface). The Metrics proposed aimed to contribute with the assessment of permanent eye damage and temporary after-image effects by calculating the irradiances from various concentrating solar collector systems (e.g., heliostats, dishes, troughs, receivers).

Toet et al., in 2013, provided the reversible and irreversible effects of visible light on human eyes and defined the requirements for effective optical measures, but the study didn't take place on a solar facility.

After a year, Ho et al. (2014, 2015), evaluated the glare in the solar power plant Ivanpah located in the United States, due to the existence of reports submitted by pilots and air traffic controllers about the glare originated from the facility. The fact drove to the evaluation and quantification of the flux of irradiance in the facility in order to identify the potential ocular impacts of the glare source at distance ranging from 2 to 32 km. The assessment was based in the quantification of the irradiance in photographs processed using the PHLUX method. The results showed the intense glare caused by the heliostats' surfaces in standby mode could cause an after-image effect (up to a distance of 10 km). In the case of the receiver's surface, the glare had a low potential to cause the same effect.

Samaniego et al. (2012, 2015) evaluated the eye hazards due to solar radiation exposure in a CRS experimental facility in Mexico. Basically the levels of the solar radiation flux were simulated with the National Renewable Energy Laboratory (NREL) software ¨SOLTRACE ¨ (http://www.nrel.gov/csp/soltrace.html). The actions of looking directly to the surface of the heliostats, and looking directly the receiver's surface were estimated with the metrics proposed by Ho et al. (2011). The data was compared with the maximum permissible limits showed in previous studies. The results showed that permanent damage (e.g., retinal injuries) and momentary vision loss (after-image effect) could occur. In the situation when a person looks directly to a single heliostat' surface, the reflected irradiance has enough potential to cause damage in the retina in a range of 300 m. Same authors, one year later, (Samaniego et al., 2016) developed a review about "Occupational exposures to solar radiation in concentrated solar power systems: A general framework in central receiver systems", where it was provided information about solar radiation, health impairments, international institutions guidelines, methodologies of assessment, among other aspects, that enable an individual to execute a risky task under the safest possible conditions.

In 2015, González-Pardo et al., focused on the evaluation of glare that produces permanent eye damage and temporary flash blindness by adding a new step in order to adapt the methodology provided by previous analyses performed by other authors. The study was carried on the "Vertical Heliostat Field" (VHF) located in the region of Madrid. The results showed that values for temporary blindness suggested the need of preventive measures in order to avoid solar reflections from bright surfaces.

2. Methodology

Ho et al. (2009) and Brumleve (1984) proposed short-term exposure parameters in order to assess the bright light sources in CSP installations. In those studies two variables were defined as necessary for the ocular impact assessment:

(i) The retinal irradiance (E_r).
(ii) The subtended angle (size) of the glare source (ω).

The retinal irradiance can be calculated from the total power entering the pupil and the retinal image area, as follows:

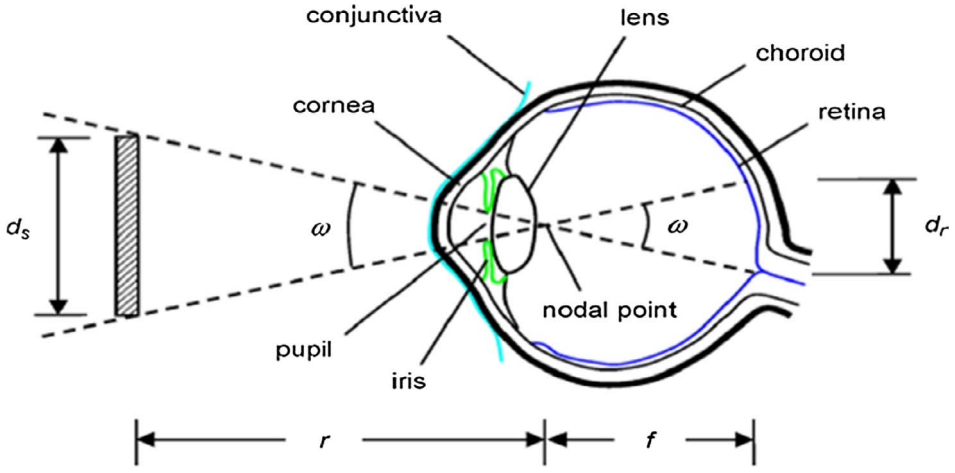

Fig. 1. Image projected onto the retina of the eye. Taken from Ho et al., 2011.

$$\omega = d_s/r \quad (1)$$

$$d_r = f\omega \quad (2)$$

where $d_r = f\omega$, is the product of focal length of the eye ($f = 0.017$ m) by the subtended angle (ω, in radians) (Sliney and Freasier, 1973); d_s is the source size, and r refers to the distance between the eye and the source (Ho et al., 2009) [Fig. 1].

The power entering to the pupil (E_r, retinal irradiance) is calculated as the product of the irradiance in the frontal plane of the cornea, E_c (W/m^2), and the pupil area (d_p). The power in the retina is divided by the retinal image area (d_r) and multiplied by the transmission coefficient ($\tau \sim 0.5$, as indicated by Brumleve (1984)), i.e.:

$$E_r = E_c\left(\frac{dp^2}{dr^2}\right)\tau \quad (3)$$

where d_p is the daylight adjusted pupil diameter (~2 mm) (Brumleve, 1984).

By substituting Eqs. ((2) into (3)) gives:

$$E_r = E_c\left(\frac{dp^2}{f^2\omega^2}\right)\tau \quad (4)$$

The calculated irradiances and thresholds for the determination of the ocular impacts are based in the solar spectral distribution (ASTM G 173-03) within the visible spectrum (from 380 to 800 nm, according to Ho et al., 2011). A potential risk to the eye scenery resides in the moment when ω increases and the safe threshold for E_r proportionally decreases. In other words, the permanent eye damage might occur when the delivery of power into the retina occurs in a larger amount. This happens because a larger subtended angle of a source ends in a larger retinal image, so it ends delivering an amount of power that the retina cannot easily dissipate.

The threshold for the burn in the retina can be represented by $E_{r,\ burn}$ (W/cm^2) and, according to Brumleve (1984), should be delimited by the threshold limit:

$$E_{r,burn} = \frac{0.118}{\omega}, for\ \omega < 0.118\ rad E_{r,burn} = 1; for\ \omega \geqslant 0.118\ rad \quad (5)$$

As the burns in the retina, the temporary blindness, caused by a flash (after-image effect), depends also on the size of the subtended angle of the source but differs on the severity of the impact. For instance, for a given irradiance, lesser or greater source ends in smaller/bigger after-image effect. Several authors (e.g., Brumleve, 1984; Ho et al., 2009) affirm that the size of the after-image and the impact is minor with small angles (ω). The potential threshold of after- image ($E_{r,\ flash}$) (W/cm^2) can be calculated as indicated in Eq. ((6)):

$$E_{r,flash} = \frac{3.59x10^{-5}}{\omega^{1.77}} \quad (6)$$

Once the values of E_r are determined, they can be compared with security metrics as provided by Ho et al. (2011).

The potential impacts in the eye for short-term exposures are resumed in [Fig. 2], where three potential risks of impact regions are defined:

1. The risk of permanent damage to the eye or retinal burn in 0.15 s (typical average time of blink response)
2. Potential for a temporary after-image effect
3. Low potential to produce after-image effect

The retinal irradiance, E_r, caused by the action of looking directly to the sun (~8 W/cm^2), in Fig. 2, is settled up as a situation of reference and is delimited by the parameters: $\beta = 9.4$ mrad, $\omega = 0.0094$ rad, $E_{DNI} = 0.1$ W/cm^2, $d_p = 0.002$ m, $f = 0.017$ m, and $\tau = 0.5$.

It is important to notice the fact that the quantified metrics and retinal irradiance estimations do not consider all the factors and situations, e.g., the atmospheric attenuation, the situation of a person is wearing sun glasses, other human factors and behaviors, and also multiple beams from adjacent receiver (s) (Brumleve, 1984).

2.1. Specular reflections from the surface of the heliostats

Situations where the surface of the mirrors is in a position that allow the reflection of the sun to locations other than the receiver may occur. Those situations can lead to glint and glare hazards. In order to evaluate the situations under the conditions to produce the largest beam irradiance, some assumptions should be made, according to Ho et al. (2011).

Such assumptions will be considered for the calculations of the beam irradiance (E_{beam}), expressed in W/cm^2, as given in (7), which is defined as the irradiance outside the eye based on the reflection coefficient, or mirror reflectivity, (ρ), and the area of concentration ratio (C) (8).

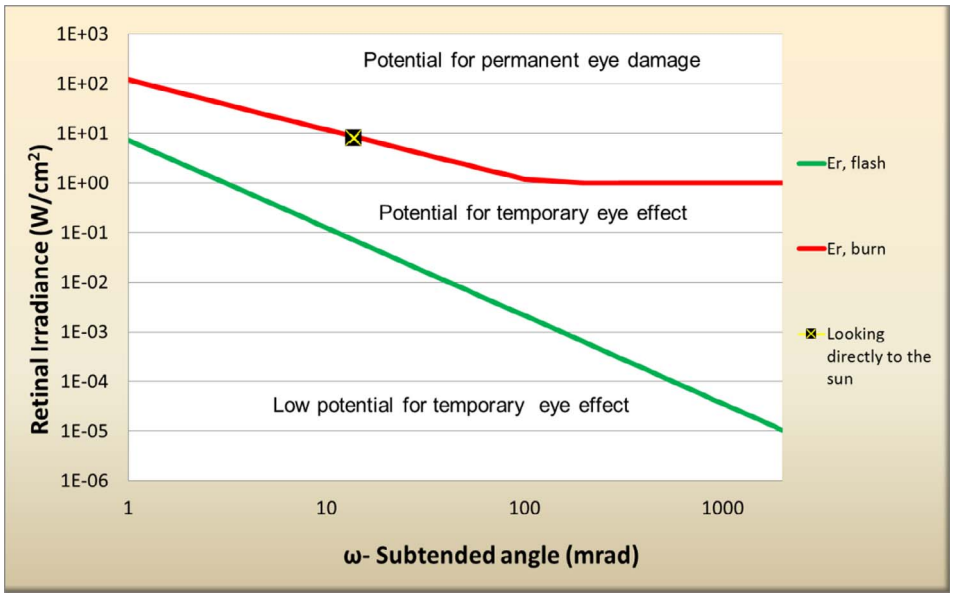

Fig. 2. Potential impacts represented as a function of the subtended angle..
Adapted from Ho et al. (2011)

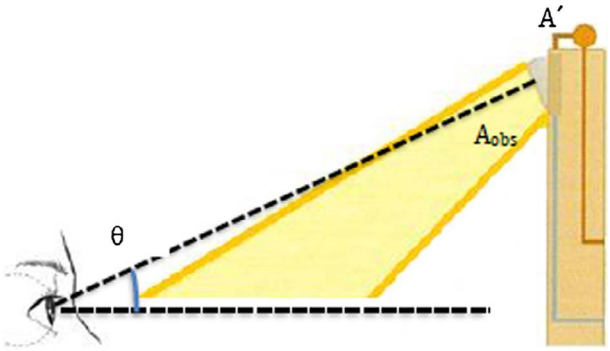

Fig. 3. Observer interaction with the receiver. Taken from Samaniego et al. (2012).

$$E_{beam} = \rho E_{DNI} C \tag{7}$$

$$C = \left(\frac{x\beta}{D_h} + |\frac{x}{b} - 1|\right)^{-2} \tag{8}$$

In Eq. (7), E_{DNI} is the direct normal irradiance at the Earth's surface (0.1 W/cm^2) (Ho et al., 2011); ρ is assumed equal to 0.92 (Ho et al., 2011). Additionally, b is the focal length (set as $b = \infty$ for a flat mirror), x is the distance between the mirror and the observer, being β the total beam divergence angle (assumed as 9.4 mrad, according to Ho et al., 2011), and D_h is the effective diameter of the mirror (calculated from the total reflective surface of the mirror).

The size of the sun image that is reflected in the surface of the heliostats is different from the one observed by the individual (Ho et al., 2011). Therefore it is necessary to calculate the size of the reflected sun image in the mirror that is being observed, in order to determine the retinal irradiance (E_r) and the subtended angle of the source (ω).

According to Ho et al. (2011) it must to be taken into consideration the spot size of the image, proportional to the measured irradiance ($E_{beam} = E_c$), which is projected in the surface and observed by a person at a given distance (x).

The concentration ratio "C", is proportional to the area of the reflected spot image (A_{spot}) on the flat mirror viewed by the observer. Therefore, C is also equivalent to the square of the diameter's ratio of the reflected area on the mirror (A_{spot}).

$$C = \frac{A_{spot}}{A_{spot,flat}} = \left(\frac{d_{spot}}{d_{spot,flat}}\right)^2 = \left(\frac{x\omega_{spot}}{x\beta}\right)^2 \tag{9}$$

where ω_{spot} is the subtended angle of the reflected image on a mirror, as observed from a given distance, and ($x\beta$) is the diameter of the reflected sun image observed at a x distance away from an infinitely large flat mirror.

The subtended angle, of the reflected image on a mirror as observed from a given distance, it is express by (10):

$$\omega_{spot} = \beta\sqrt{\frac{E_{beam}}{\rho E_{DNI}}} \tag{10}$$

where $E_{beam} = E_c$.

The retinal irradiance (from specular reflections), in (11), is obtained from using (10) in (1), (2) and (3)

$$E_r = \frac{\rho E_{DNI} d_p^2 \tau}{f^2 \beta^2} \tag{11}$$

Referring to the Eq. (11), Ho et al. (2011) in their work, indicate that:

"The retinal irradiance does not depend on distance from the source (neglecting atmospheric attenuation). As the distance increases, both the power entering into the pupil and the retinal image area (which is proportional to the square of the subtended source angle) decrease at the same rate. Therefore, the retinal irradiance, which is equal to the power entering to the pupil dived by the retinal image area, is independent of distance"

In the application of the methodology for the evaluation of ocular impacts, the Eqs. (13) are used to convert E_c into E_r; where ω is represented by the ω_{spot} (10). Eq. (11) can be used for comparisons to the safe retinal irradiance levels in Fig. 2.

2.2. Diffuse reflections from the receiver

The receiver, located on the top of the tower, is designed to absorb the solar radiation coming from the heliostats field (Brumleve, 1984) and in order to assess the action of seeing the reflection of bright light coming from it and its impact to eyes, the receiver surface can be interpreted as a diffuse source. Samaniego et al. (2012) proposed a way to evaluate the reflected irradiance coming from diffuse sources based on the methodology proposed by Ho et al. (2011).

The angular size of the source is determined by the effective area reflected on the receiver surface which is seen by the observer [Fig. 3].

The effective area seen by the observer (A_{obs}) can be calculated using (12), where the angle between the tower and the observer depends on the distance between them and the tower height.

$$A_{obs} = A'\cos\theta \tag{12}$$

being A_{obs} the area seen by the observer, θ the angle, and A' the area of the reflecting surface.

Once the total illuminated area is known, the reflected irradiance (E_{ref}) can be calculated (13) by multiplying it by the reflection coefficient ρ (0.8 to 0.2) and the amount of irradiance seen by the observer (E'):

$$E_{ref} = \rho E' \tag{13}$$

However, there is a difference between the total reflected radiation and the total amount of radiation outside the eye (E_c in W/cm^2). The main reason is the distance and the angle in which the observer is located with respect to the receiver. The irradiance outside of the cornea is defined by:

$$E_c = I_{ref} A' \frac{X_{obs}}{(z_{obs}^2 + X_{obs}^2)^{\frac{3}{2}}} \tag{14}$$

where $I_{ref} = \frac{E_{ref}}{\pi}$, due to the circular shape of the image.

On the other hand, the quantity of irradiance (per cm^2) that enters through the pupil (E_r) is equal to the multiplication of energy that is outside of the cornea by the area of the pupil (A_p) for a certain distance "r_{obs}" (location of the observer) divided by the area seen by the observer.

$$E_r = \frac{E_c A_p \tau \, r_{obs}^2}{A_{obs} f^2} \tag{15}$$

Here the transmission coefficient (τ) is equal to 0.5 and the focal distance of the eye (f) is equal 0.017 m (Ho et al., 2011).

Eq. (15) refers to the amount of radiation on the retina produced by a single heliostat. Therefore, the amount of reflected irradiance coming from **n** heliostats in the field and reaching the retina is determined by an equivalent area (A_{equiv}) for an equivalent irradiance (E_{equiv}) as follows:

$$A_{equiv} = \sum_{i=1}^{n} \frac{nA'_{i-n} nE'_{i-n}}{nE'_{i-n}} \tag{16}$$

The equivalent irradiance, E_{equiv} , is represented by the sum of the amounts of reflected irradiance coming from the heliostats. As it can be seen in:

$$E_{equiv} = \sum_{i=1}^{n} nE'_{i-n} \tag{17}$$

3. Case of study and results

Like many other countries, Mexico has a considerable potential for applications in solar energy due to the high amounts of solar radiation over its territory, in particular in the states located in the north region, namely Sonora, Baja California, and Chihuahua. The NREL, in its website (http://maps.nrel.gov/swera), includes a geographic information system, which displays worldwide information of direct normal solar radiation [Fig. 4]. The state of Sonora is indicated as having one of the highest solar irradiance levels in the whole country (Arancibia-Bulnes et al., 2014).

A study over three regions of Sonora, based on beam solar radiation measurements, showed that the capital of Sonora, Hermosillo, has a beam normal solar radiation of 7.8 kWh/m^2/day. Furthermore, in that city, the number of hours in a day with irradiance above the average value exceeds 10 h, which is an excellent value for concentrated solar energy uses (Arancibia-Bulnes et al., 2014).

The present study was conducted in the Experimental Field of Heliostats (initials CPH, in Spanish) [Fig. 5], located in Hermosillo, Sonora, México. Such scientific and technological research installation is supervised by the University of Sonora and by the National Autonomous University of Mexico. The CPH consists of a field of 15 heliostats, with a total surface of 36 m^2 (Iriarte, 2013), a tower 36 m height, and a control room. The heliostats installed on the field allow reaching a solar radiation concentration factor of 25 and an estimated thermal power of 2 MWt (Samaniego et al., 2012).

The workers of CPH have the following tasks:

1. Operation of the heliostats field: Verification of the operation of the field, heliostat calibration routines and calibration parameters, feedback control system, running the control and monitoring system.
2. Monitoring system (direct, diffuse, global measurements): Cleaning and maintenance of the equipment located at the top of the tower (gardon gauge, pyranometer and pyrheliometer), supervising the equipment operation and backup the stored data.

The monitoring system was designed in two stages; the first one, dealing with the acquisition and recording of data and, the second one, with the processing and analysis of the information in the central control system. The first stage was installed on the hardware cRIO-9074 controller with the FTP- Server enabled for access to historical information from the system module. The system was installed in the upper part of the tower with the function of obtaining measurements of

Fig. 5. Experimental installation CPH. Taken from Samaniego et al. (2012).

Table 1
Solar irradiance over a year.

Temperature °C	Month	Irradiance peak flux in a day (W/m^2)	Averages of maximum levels of irradiance per month (W/m^2)
29.90	January	998.07	882.70
32.61	February	1012.75	935.53
25.33	March	998.15	894.92
30.87	April	996.89	895.19
34.21	May	961.37	898.77
38.62	June	940.79	890.76
36.84	July	897.27	889.23
39.33	August	953.56	906.28
36.62	September	918.91	900.60
35.52	October	971.78	930.13
26.09	November	1005.69	931.87
25.19	December	968.43	851.51
	Average	**968.64**	

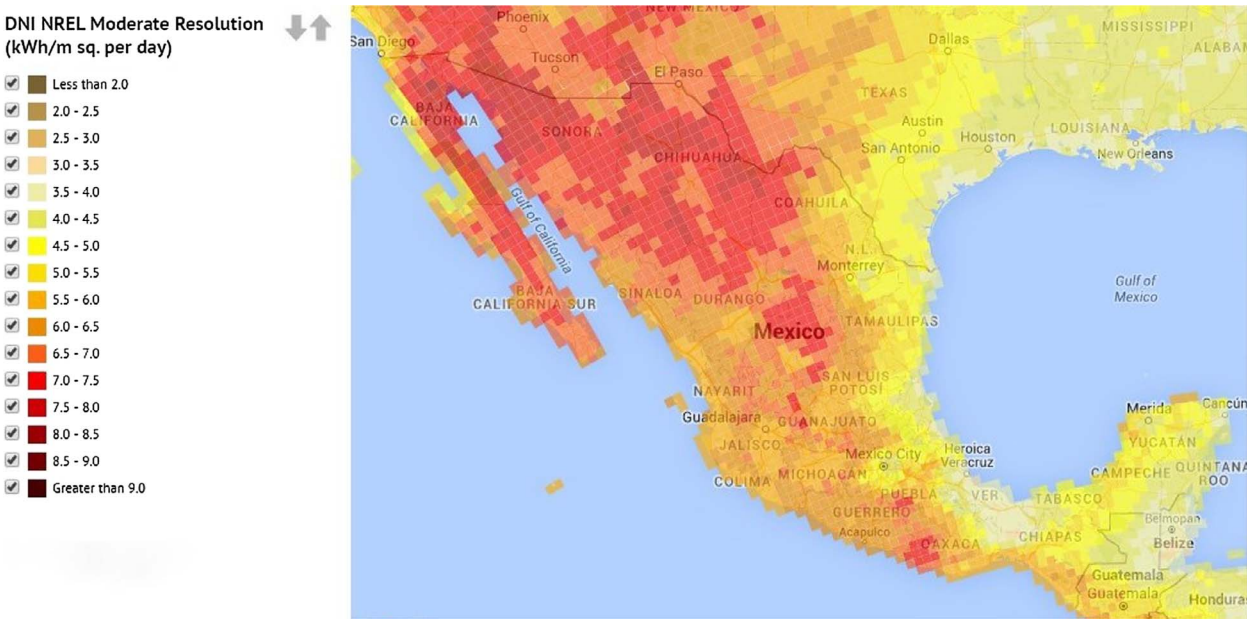

Fig. 4. Direct normal irradiance in Mexico (NREL: http://maps.nrel.gov/swera).

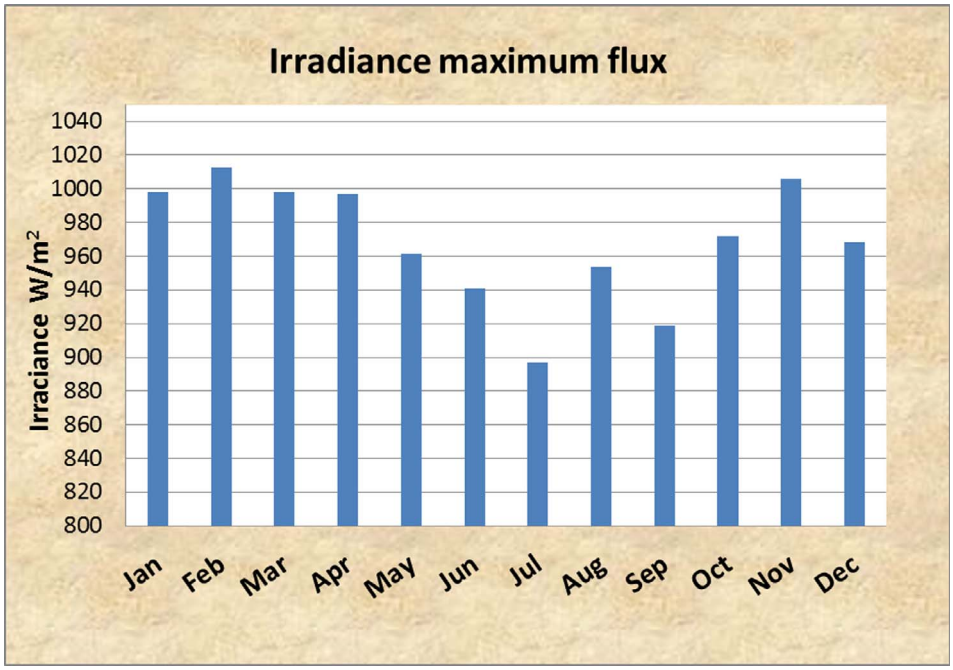

Fig. 6. Maximum irradiance fluxes per month.

Table 2
Conversion of E_c into the irradiance that enters to the eye (E_r).

E_c	E_{DNI}	β	W_{spot}		E_r		$E_{b\ urn}$	$E_{r\ flash}$
998.073	1000	0.0094	0.0098	9.791	72055.025	7.206	12.052	1.292
1012.752	1000	0.0094	0.0099	9.862	72055.025	7.206	11.965	1.276
998.148	1000	0.0094	0.0098	9.791	72055.025	7.206	12.052	1.292
996.891	1000	0.0094	0.0098	9.785	72055.025	7.206	12.059	1.294
961.375	1000	0.0094	0.0096	9.609	72055.025	7.206	12.280	1.336
940.787	1000	0.0094	0.0095	9.506	72055.025	7.206	12.414	1.362
897.270	1000	0.0094	0.0093	9.283	72055.025	7.206	12.711	1.420
953.560	1000	0.0094	0.0096	9.570	72055.025	7.206	12.330	1.346
918.910	1000	0.0094	0.0094	9.394	72055.025	7.206	12.561	1.390
971.783	1000	0.0094	0.0097	9.661	72055.025	7.206	12.214	1.323
1005.687	1000	0.0094	0.0098	9.828	72055.025	7.206	12.007	1.284
968.431	1000	0.0094	0.0096	9.644	72055.025	7.206	12.235	1.327

solar radiation and weather conditions (Iriarte, 2013).

The probes, connected to NI cRio-9074 hardware and used in the measurements of diffuse radiation, direct irradiation, global radiation and irradiance, are:

1. Gardon Gauge: It's a sensor designed to measure the flux density of radiation (Pitts et al., 2006).
2. Pyranometer: It is an instrument that measures the global solar radiation (direct plus diffuse radiation) in a horizontal plane (Kalogirou, 2009; Robinson, 1966, cited in CEDECAP, 2003, pp.13).
3. Pyrheliometer: It is an instrument to measure the flux of direct solar radiation at normal incidence. This instrument is a type of telescope that follows the solar movement (Iqbal, 1983; Kalogirou, 2009).

The sampling rate of the various variables (global, diffuse, and direct radiation) was 1 Hz. After a period of 60 s, the average of each variable was computed and stored into files. Those files were named based on the date, and new files were created every time the file size exceeded three megabytes. The measurements selected, for the present study, were those obtained during a working period between 9 am and 5 pm, on each day, and processed by the monitoring system.

The corresponding peak irradiance fluxes of each month are presented in Table 1, where it can be seen that the highest solar irradiance, in a month, ranges from a minimum of 897 to approximately 1013 W/m^2.

In Fig. 6, it can be noticed a diminution of the beam irradiance during the months around July due to the fact that such period corresponds to the local rainy season of the year, when the amount of cloudiness increases, despite of being summer there.

The irradiance measurements were assessed following the methodology proposed by Ho et al. (2011), as explained previously, in order to compare the short-term exposure of specular reflections from the surface of the heliostats against the safety threshold limits presented already in Fig. 2. The parameters were defined as: $\beta = 9.4$ mrad, $\rho = 0.92$, $E_{DNI} = 1000$ W/m^2, $d_p = 0.002$ m, $f = 0.017$ m, and $\tau = 0.5$ (Brumleve, 1984; Ho et al., 2009, 2011).

The results, in Table 2, show a retinal irradiance -E_r- of about 7.21 W/cm^2 which is close to the threshold of 8 W/cm^2 (Ho et al., 2011) that represents the irradiance that enters into the eye of a person staring at the sun and which has a considerable potential to damage the eye in a permanent way.

In Fig. 7, the actions of looking directly at the sun and looking directly at surface of the heliostats are compared with the safety levels. Based on measurements performed within a work shift of 8 h (9 am to 5 pm) over a year, the results revealed that the environmental conditions have the potential to cause after-image effect in momentary

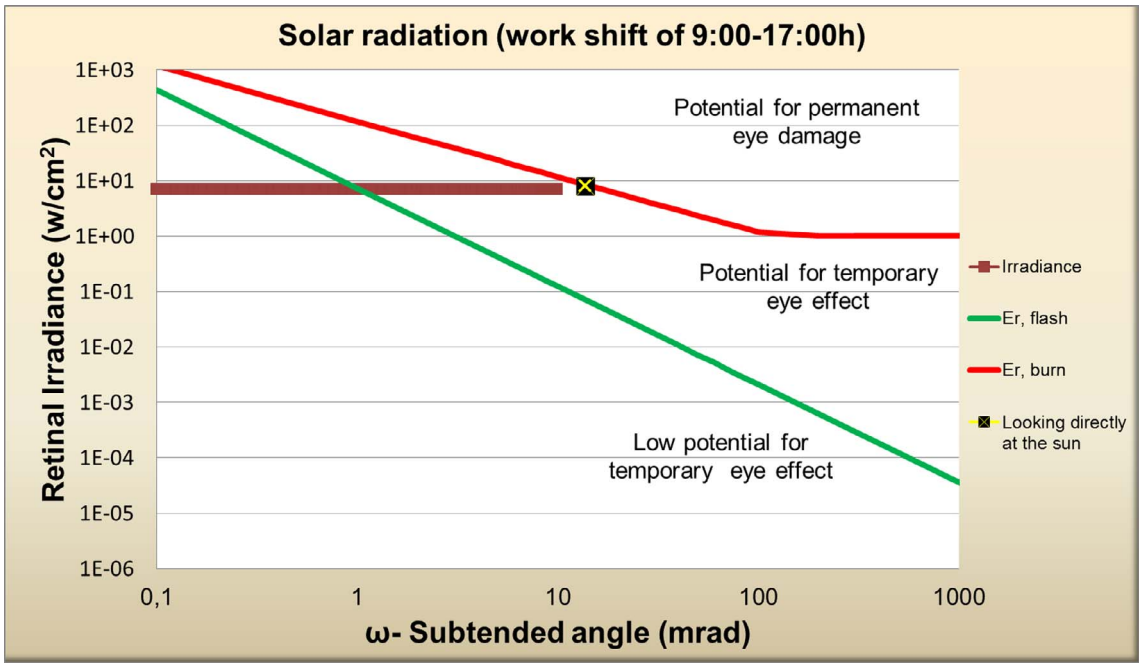

Fig. 7. Potential impacts represented in function of the subtended angle.

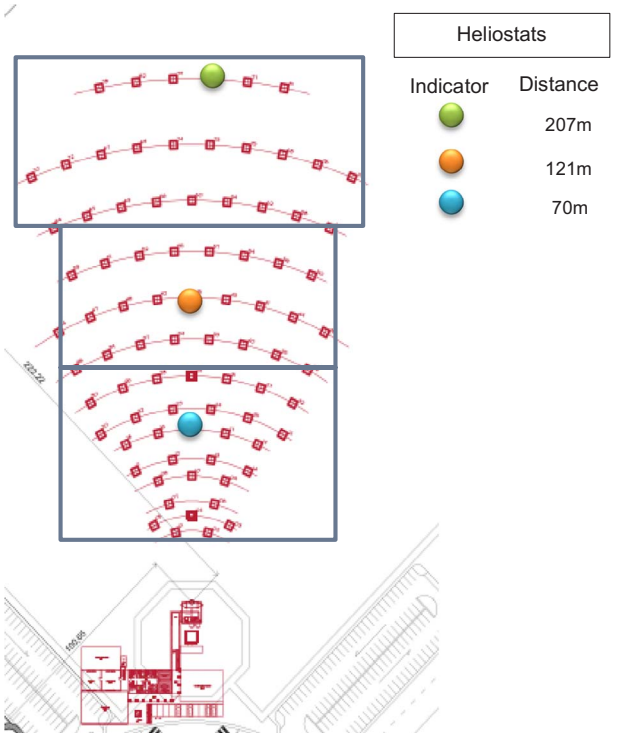

Fig. 8. Map of the groups of heliostats in the experimental field..
Adapted from Samaniego et al. (2012)

exposures, even though not sufficient potential to cause permanent eye damage.

In the design of the case for analyzing the diffuse reflection from the receiver, one person (1.65 m average height) is supposed to be looking at the receiver surface reflecting the bright light of the entire field (composed by 82 heliostats). The highest flux of irradiance was registered around 1 pm during the warmest day of the year; where the direct normal irradiance was 1012.75 W/m^2. The parameters that represent the characteristics of the facility are: E_{DNI} = 1000 W/m^2, receiver of 4 m^2 area with a reflectivity of 0.2 and the height of central tower 27 m.

The analytical model of diffuse reflections evaluates the total reflected irradiance coming from the bright source which is represented by an equivalent irradiance by using (17); based on the results of the appliance of (15). Therefore in the evaluation, three heliostats at different distances, Fig. 8, were chosen and its results were reproduced as representative information of the equivalent irradiance of each group of a total of three. The selection of the heliostats for evaluation in the study was led by strategic decision based on its distance from the central tower.

The group 1 was composed by 32 heliostats at a representative distance from the receiver of 70 m. The 25 heliostats of group 2 were representing the fringe located at 121 m from the tower and the last group of 25 heliostats at distance of 207 m. It is supposed that the person is seeing the 82 bright images overlapping in one point on the receiver. Therefore, it is hypothetical determined that the location of this individual is far enough to see the entire field of heliostats reflecting the solar radiation from receiver.

Since the total amount of reflected radiation differs from the total amount of radiation outside the eye due to the distance and the angle in which the observer is located respect to the receiver, the evaluation of the irradiance outside the eye (E_c) as a function of the distance was made [Fig. 9].

It can be noticed, in Fig. 9, that the irradiance outside the eye decreases as the distance increases. This happens because the image of the reflected bright area reduces at large viewing angles. Besides the angle and distance, the receiver reflectivity could affect the amount of E_c. If the receiver is replaced by another one with higher reflectivity (e.g. 0.8), an considerably increment of the radiation in front of the eyes (within 100 m) occurs [Fig. 10].

After obtaining the irradiance that enters into the eye from each group of heliostats reflecting the sunlight on the receiver and its equivalent irradiance, a comparison against the safety limits of exposure is shown on Fig. 11.

The results revealed that the short exposure to diffuse reflected irradiance, coming from a receiver with reflectivity of 0.2, has a low potential to cause a temporary effect as after-image effect in a person.

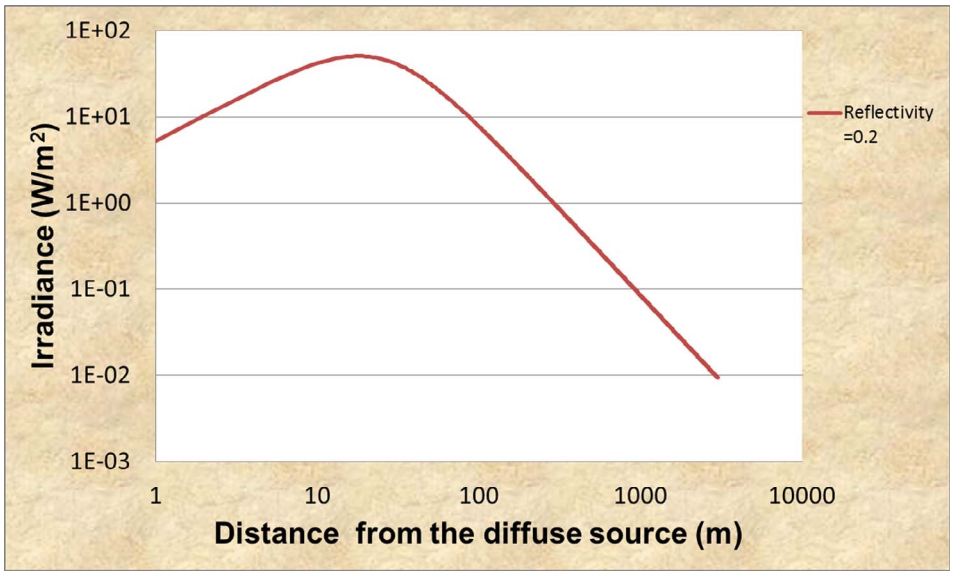

Fig. 9. Irradiance outside of the cornea as a function of the distance between the observer and the diffuse source.

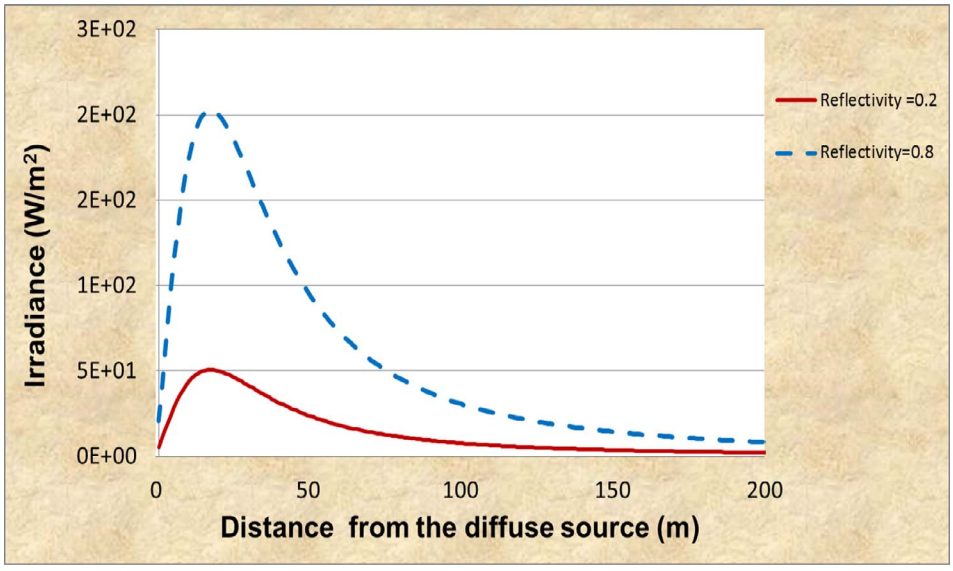

Fig. 10. Irradiance outside of the cornea as a function of the distance from the diffuse source with different reflectivity.

4. Recommendations

The main objective in suggesting preventive measures is to reduce to the minimum the ocular exposure to solar radiation. In order to reduce the risk of the glint and glare and increase the visual perception, it is needed to:

- Avoid staring at bright surfaces within the solar installation. Prolonging the period of time of eye staring before the blinking effect (avoiding reaction of the eye) will bring effects and side effects to human health.
- Advising the surroundings. The solar facilities should put sings on the near surroundings in order to spread the awareness of glare and glint to individuals or drivers passing by the solar installations. Those facilities which aren't physically materialized or they are on a project state level should take into consideration the location of the facility.
- Ocular protection. UV protective eyewear is frequently used to reduce glare by decreasing the luminance of visible radiation reaching the eye. The selection of the ocular protection needs to be based on the intensity and characteristics of the bright source, distance between the viewer and the bright source and time of exposure (Knave et al., 2001; Vecchia et al., 2007).
- Implement protection policies and monitoring program. In order to control health hazards to outdoor exposure, the monitoring program should include information about:
  - Global solar UV index (UVI). UVI describes the level of solar UV radiation at the Earth's surface. It could be monitored by using the UVI local forecast. The values of the index range from 0 to 11 + where higher the index value, greater is the potential for damage and the lesser the time for harm to occur (WHO, 2002).
  - Self-protection and behavior
  - Shelter in shades

Training and education of employees about safety and the importance of prevention providing information about protection policies, preventive measures, limits of exposure and symptoms of hazardous effects on health and its identification.

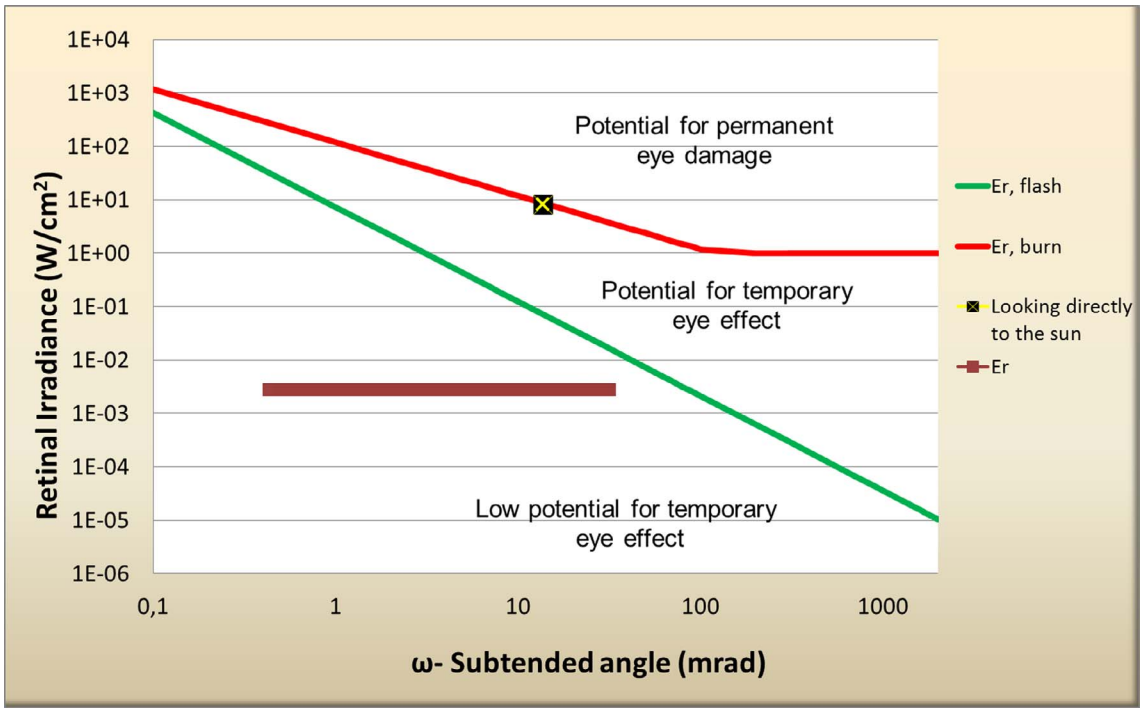

Fig. 11. The action of looking at the receiver reflecting the irradiance of 82 heliostats.

5. Conclusions

The present work aims to contribute with information about eye exposures to solar radiation in CRS installations for the development of standard procedures, in the future, in order to ensure the safety in the solar industry workforce.

To accomplish such objective, field data measurements of solar radiation were conducted, during nearly a year, in a solar experimental facility located in Mexico.

The analysis, based on such real data, provided relevant information about the actions of looking directly at the surface of the heliostats and looking directly to the surface of the receiver. In the case of seeing the solar radiation reflected on the receiver there exist a low potential to cause a temporary effect on the eye. This happens because the irradiance outside the eye decreases while the distance increases, in other words, the image of the reflected bright area on the receiver reduces at large viewing angles. On the other hand, the results revealed a potential temporary effect (after-image) when a person is looking at the surface of the heliostat. Even though the after-image effect is classified as reversible impact, in other words, physiologically healed with time, those situations may lead to secondary effects (headache, degradation of vision, dazzle and temporary loss of the vision, dizziness and vertigo) or accidents at work. Therefore, it would be desirable to mitigate the situations of risk.

Clearly further studies are needed to understand more in deeep the ocular exposures to solar radiation. The reproduction of this study on a comecial solar facility, the establishment of security measures, training procedures, monitoring systems and methods of evaluation adapted to the solar industry requirements are highly recommended. Address solar exposures will influence in the effects on health prevention and costs in health care.

Acknowledgments

The presented work is framed under the Energy for Sustainability Initiative of the University of Coimbra and LAETA (Associated Laboratory for Energy, Transports and Aeronautics) Project Pest- E/EME/LA0022/201. The first author carried out the work in the framework of a Ph.D. grant [314149] supported by the Mexican government foundation for Science and Technology, CONACyT, which she sincerely acknowledges. The authors of the present work are also thankful to the staff and research team of the experimental field of heliostats located in the Solar Platform of Hermosillo (PSH in Spanish), Sonora, Mexico, for the support and contribution to this paper.

References

Arancibia-Bulnes, C.A., Peón-Anaya, R., Riveros-Rosas, D., Quiñones, J.J., Cabanillas, R.E., Estrada, C.A., 2014. Beam solar irradiation assessment for Sonora, Mexico. Energy Proc. 49, 2290–2296.

Ashouri, M., Vandani, A.M.K., Mehrpooya, M., Ahmadi, M.H., Abdollahpour, A., 2015. Techno-economic assessment of a Kalina cycle driven by a parabolic Trough solar collector. Energy Convers. Manage. 105, 1328–1339.

Astolfi, M., Binotti, M., Mazzola, S., Zanellato, L., Manzolini, G., 2017. Heliostat aiming point optimization for external tower receiver. Solar Energy 157, 1114–1129.

Behar, O., Khellaf, A., Mohammedi, K., 2013. A review of studies on central receiver solar thermal power plants. Renew. Sustain. Energy Rev. 23, 12–39.

Brumleve, T.D., 1977. Eye Hazard and Glint Evaluation for the 5-MW1 Solar Thermal Test Facility. Sandia National Laboratories for the US Department of Energy, available from the National Technical Information Service, Springfield, VA.

Brumleve, T.D., 1984. 10 MWe Solar Thermal Central Receiver Pilot Plant: Beam Safety Tests and Analyses, SAND83-8035. Sandia National Laboratories, United States of America.

Burlafinger, K., Vetter, A., Brabec, C.J., 2015. Maximizing concentrated solar power (CSP) plant overall efficiencies by using spectral selective absorbers at optimal operation temperatures. Sol. Energy 120, 428–438.

Carrasco, J.L., 2003. Radiaciones ionizantes y no ionizantes. Aplicaciones y riesgos. Hospital U, Málaga, [online] Available at: http://www.marcoshurvitz.com.ar/Archivos/Docen/ISFT%20190/Radiaciones%20y%20patologia.pdf (accessed 15.09.17).

CEDECAP. Centro de Demostración y Capacitación en Tecnologías Apropiadas, 2003. Atlas de energía solar del Perú, [online] .Lima, Perú. Available from: http://www.cedecap.org.pe/uploads/biblioteca/80bib_arch.pdf (accessed 15.09.17).

Corona, B., Cerrajero, E., López, D., San Miguel, G., 2016. Full environmental life cycle cost analysis of concentrating solar power technology: contribution of externalities to overall energy costs. Sol. Energy 135, 758–768.

Diffey, B.L., 1991. Solar ultraviolet radiation effects on biological systems. Phys. Med. Biol. 36 (3), 299.

ECLIMP Termosolar, services 2016. Available at: < http://termosolar.ecilimp.com/servicios.html > (accessed 15.09.17).

Franck, D., Walzer, S., Chernin, O., 2009. Assessment and resolution of potential optical safety hazards from a power tower. Proc. Solar PACES 15–18.

Gauché, P., Rudman, J., Mabaso, M., Landman, W.A., von Backström, T.W., Brent, A.C., 2017. System value and progress of CSP. Solar Energy 152, 106–139.

González-Pardo, A., González-Aguilar, J., Romero, M., 2015. Analysis of glint and glare produced by the receiver of small heliostat fields integrated in building façades. Methodology applicable to conventional central receiver systems. Sol. Energy 121, 68–77.
Hamilton, J., 2011. Careers in solar power. Green jobs: solar power. The Bureau of Labor Statistics. [online] Available at: < http://www.bls.gov/green/solar_power/solar_power.pdf > (accessed 15.09.17).
Ho, C.K., 2017. Advances in central receivers for concentrating solar applications (No. SAND–2017-6158J). Sandia National Laboratories (SNL-NM), Albuquerque, NM (United States). Sol. Energy 152, 38–56.
Ho, C.K., Ghanbari, C.M., Diver, R.B., 2009. Hazard analyses of glint and glare from concentrating solar power plants. Proc. Solar PA-CES 15–18.
Ho, C.K., Ghanbari, C.M., Diver, R.B., 2011. Methodology to assess potential glint and glare hazards from concentrating solar power plants: analytical models and experimental validation. J. Sol. Energy Eng. 133 (3), 031021.
Ho, C.K., Sims, C.A., Christian, J.M., 2014. Evaluation of Glare at the Ivanpah Solar Electric Generating System. Ivanpah Solar Electric Generating System California Energy Commission (07-AFC-5C) Bureau of Land Management (CACA-48668, 49502, 49503, and 49504) Condition of Certification TRANS-3.
Ho, C.K., Sims, C.A., Christian, J.M., 2015. Evaluation of glare at the Ivanpah solar electric generating system. Energy Proc. 69, 1296–1305.
Ho, C.K., 2011. Observations and Assessments of Glare from Heliostats and Trough Collectors: Helicopter Flyover and Drive-By Sightings: Solarpaces. Cantabria, Spain.
IEA, 2014. Technology Roadmap: Solar Thermal Electricity. International Energy Agency. [online] Available at: < https://www.iea.org/publications/freepublications/publication/technologyroadmapsolarthermalelectricity_2014edition.pdf > (accessed 15.09.17).
International Commission on Non-Ionizing Radiation Protection, 2010. ICNIRP statement—protection of workers against ultraviolet radiation. Health Phys. 99 (1), 66–87.
International Commission on Non-Ionizing Radiation Protection, 2004. Guidelines on limits of exposure to ultraviolet radiation of wavelengths between 180 nm and 400 nm (incoherent optical radiation). Health Phys. 87 (2), 171–186.
Iqbal, M., 1983. An introduction to solar radiation: solar radiation measuring instruments, 1st ed., ACADEMIC PRESS: Canada 12, 1983, pp. 335–362.
Iriarte C., 2013. Automatización de Sistema de Control para Campo De Helióstatos. M.C. Instituto tecnológico de Chihuahua División de Estudios de posgrado e Investigación [in Spanish].
Jamel, M.S., Abd Rahman, A., Shamsuddin, A.H., 2016. Novel integrations of molten salt cavity tubular solar central receiver with existing gas-fuelled conventional steam power plants. Int. J. Sustain. Energy 35 (1), 21–32.
Kalogirou, S., 2009. Solar Energy Engineering: Processes and Systems. Academic Press. ISBN 978-0-12-374501-9 1, 533.
Kattke, K., Vant-Hull, L., 2012. Optimum target reflectivity for heliostat washing. In: SolarPACES Conference, Marrakech, Morocco.
Knave, B., Mild, K.H., Sliney, D.H., Matthes, R., Repacholi, M.H., Grandolfo, M., 2001. Enciclopedia de salud y seguridad en el trabajo: Radiaciones no ionizantes, 3.49, pp. 1–10 (in Spanish).
Kwan-Hoong Ng, 2003. Non-Ionizing Radiations – Sources, Biological Effects, Emissions and Exposures: proceedings of the international conference on Non- Ionizing Radiation, UNITEN, ICNIR2003. [Online] Available at: < http://www.who.int/peh-emf/meetings/archive/en/keynote3ng.pdf > (accessed 15.09.17).
Mekhilef, S., Saidur, R., Safari, A., 2011. A review on solar energy use in industries. Renew. Sustain. Energy Rev. 15 (4), 1777–1790.
Oncel, S.S., 2017. Green energy engineering: opening a green way for the future. J. Cleaner Prod. 142, 3095–3100.
Osterhaus, W.K., 2005. Discomfort glare assessment and prevention for daylight applications in office environments. Sol. Energy 79 (2), 140–158.
Pitts, W.M., Murthy, A.V., de Ris, J.L., Filtz, J.R., Nygård, K., Smith, D., Wetterlund, I., 2006. Round robin study of total heat flux gauge calibration at fire laboratories. Fire Saf. J. 41 (6), 459–475.
Reyes-Belmonte, M.A., Sebastián, A., Romero, M., González-Aguilar, J., 2016. Optimization of a recompression supercritical carbon dioxide cycle for an innovative central receiver solar power plant. Energy 112, 17–27.
Samaniego, D.R., Arancibia, C.A., León, J., 2012. Estimación de riesgos oculares por reflexión de radiación solar concentrada en una instalación de torre central. In: Proceedings of the 10th International Conference on OPR, Occupational Risk Prevention, Bilbao, España (in Spanish).
Samaniego, D.R., Ferreira, A.D., Da Silva, M.G., 2015. Risk assessment in a CRS; 14th International Conference on Sustainable Energy Technologies (SET 2015), Nottingham, UK.
Samaniego, D.R., Ferreira, A.D., Da Silva, M.G., 2016. Occupational exposures to solar radiation in concentrated solar power systems: a general framework in central receiver systems. Renew. Sustain. Energy Rev. 65, 387–401.
Saur, R.L., Dobrash, S.M., 1969. Duration of afterimage disability after viewing simulated sun reflections. Appl. Opt. 8 (9), 1799–1801.
SENER, 2011. HECTOR, cleaning robot systems for heliostats. [Online] Available at: < http://www.senermar.es/EPORTAL_DOCS/GENERAL/SENERV2/DOC-cw4efc4f1de8b47es/pdfproject.pdf > (accessed 15.09.17).
Sindhu, S.P., Nehra, V., Luthra, S., 2016. Recognition and prioritization of challenges in growth of solar energy using analytical hierarchy process: Indian outlook. Energy 100, 332–348.
Sliney, D.H., 1994. Ocular hazards of light. In: Tibbitts, T.W. (Ed.), International Lighting in Controlled Environments Workshop. pp. 183–189. NASA-CP-95-3309.
Sliney, D.H., 2001. Photoprotection of the eye–UV radiation and sunglasses. J. Photochem. Photobiol. B 64 (2), 166–175.
Sliney, D.H., Freasier, B.C., 1973. Evaluation of optical radiation hazards. Appl. Opt. 12 (1), 1–24.
Toet, A., Benoist, K.W., van Lingen, J.N., Schleijpen, R.M.A., 2013. Optical countermeasures against CLOS weapon systems. In: Proc. of SPIE Vol, vol. 8898, pp. 88980L-1.
Vecchia, P., Hietanen, M., Stuck, B.E., van Deventer, E., Niu, S., 2007. Protecting Workers from Ultraviolet Radiation, vol. 14 International Commission on Non-Ionizing Radiation Protection, Oberschleißheim, Germany978-3-934994-07-2.
World Health Organization (WHO), 2002. Global solar UV index: A practical guide. [Online] Available at: < http://apps.who.int/iris/bitstream/10665/42459/1/9241590076.pdf?ua=1 > (accessed 15.09.17).
Young, L.L., 1977. Solar energy research at Sandia Laboratories and its effects on health and safety. SAND77-1412, Sandia National Laboratories, United States of America.
Zhao, Zhen-Yu, Chen, Yu-Long, Thomson, John Douglas, 2017. Levelized cost of energy modeling for concentrated solar power projects: a China study. Energy 120, 117–127.